

Published in final edited form as:

Genes Chromosomes Cancer. 2009 June ; 48(6): 480–489. doi:10.1002/gcc.20654.

Overexpression of *ZNF342* by Juxtaposition with *MPO* Promoter/Enhancer in the Novel Translocation t(17;19)(q23;q13.32) in Pediatric Acute Myeloid Leukemia and Analysis of *ZNF342* Expression in Leukemia

Kathryn S. Poland¹, Deborah L. Shardy^{2,†}, Mohammed Azim³, Rizwan Naeem³, Robert A. Krance^{2,4,5}, ZoAnne E. Dreyer^{2,4}, E. Shannon Neeley⁶, Nianxiang Zhang⁷, Yi Hua Qiu⁸, Steven M. Kornblau⁸, and Sharon E. Plon^{1,2,4,*}

¹Department of Molecular and Human Genetics, Baylor College of Medicine, Houston, TX

²Department of Pediatrics, Baylor College of Medicine, Houston, TX

³Cytogenetics/Molecular Laboratory, Texas Children's Cancer Center, Texas Children's Hospital, Houston, TX

⁴Texas Children's Cancer Center, Texas Children's Hospital, Houston, TX

⁵Cell and Gene Therapy Program, Baylor College of Medicine, Houston, TX

⁶Department of Statistics, Brigham Young University, Provo, UT

⁷Department of Bioinformatics and Computational Biology, The University of Texas M.D. Anderson Cancer Center, Houston, TX

⁸Department of Stem Cell Transplantation and Cellular Therapy, The University of Texas M.D. Anderson Cancer Center, Houston, TX

Abstract

We report a novel translocation t(17;19)(q22;q13.32) found in 100% of blast cells from a pediatric acute myeloid leukemia (AML) patient. Fluorescence in situ hybridization and vectorette polymerase chain reaction were used to precisely map the chromosomal breakpoint located on the derivative chromosome 17 at 352 bp 5' of *MPO*, encoding myeloperoxidase a highly expressed protein in myeloid cells, and 2,085 bp 5' of *ZNF342* on 19q, encoding a transcription factor expressed in human stem cells and previously implicated in mouse models of leukemia. Analysis of RNA levels from the patient sample revealed significant overexpression of *ZNF342*, potentially contributing to AML formation. This is the first report of a translocation in myeloid leukemia occurring only in the promoter/enhancer regions of the two genes involved, similar to translocations commonly found in lymphoid malignancies. Analysis of *ZNF342* protein levels in a large dataset of leukemia samples by reverse phase protein array showed that higher levels of *ZNF342* expression in acute lymphoblastic leukemia was associated with poorer outcome ($P=0.033$). In the myeloid leukemia samples with the highest *ZNF342* expression, there was overrepresentation of *FLT3* internal tandem duplication ($P=0.0016$) and AML subtype M7 ($P=0.0002$). Thus, overexpression of *ZNF342* by translocation or other mechanisms contributes to leukemia biology in multiple hematopoietic compartments.

INTRODUCTION

Acute myeloid leukemia (AML) is a heterogeneous group of malignancies characterized by rapid proliferation of immature blood cells of the myeloid lineage. AML has long been associated with chromosomal abnormalities, primarily balanced translocations, with greater than 50% of patient samples containing one or more (Arthur et al., 1989). The identification of precise breakpoint loci have led to the discovery of multiple genes involved in the formation of AML and the mapping and characterization of new translocation breakpoints is essential to further our understanding of leukemogenesis.

Here we report a novel translocation t(17;19)(q22;q13.32) in a pediatric AML patient. We have precisely mapped the translocation breakpoint and determined that on the derivative chromosome 17 the myeloperoxidase (*MPO*) promoter/enhancer region, located on 17q, is centromeric to the breakpoint and the promoter and coding region of the zinc finger transcription factor *ZNF342*, normally located on 19q, is translocated telomeric to the breakpoint.

Zfp296, the murine homologue of *ZNF342*, has 75% nucleotide similarity and both genes contain six C₂H₂-type zinc finger domains. *Zfp296* was first identified as a proviral insertion site in a BHX2 mouse with retrovirally induced myeloid leukemia (Li et al., 1999; Dear, 2000) and was later found to be common insertion site (CIS) Evi82, with insertions found upstream of *Zfp296* in multiple leukemic mice (Suzuki et al., 2002). We report here the first example of a human leukemia involving upregulation of the human ortholog, *ZNF342*, in pediatric AML and further analysis of *ZNF342* expression in a large leukemia dataset.

MATERIALS AND METHODS

Patient Samples, Cytogenetics, and Cell Lines

Patients were enrolled in protocols approved by the Baylor College of Medicine and University of Texas MD Anderson Cancer Center Institutional Review Boards that include clinical sample collection, linkage to clinical data, and banking of samples for research purposes. DNA was prepared using the QIAamp DNA blood mini kit (Qiagen, Valencia, CA, 51106), Genra PUREGENE Cell and Tissue Kit (Genra, Valencia, CA, 158788), or DNA STAT60 (IsoTex Diagnostics, Friendswood, TX, TL-4200) and RNA was prepared using the RNeasy mini kit (Qiagen, 74104) or RNA STAT60 (IsoTex Diagnostics, CS-110) according to the manufacturer's instructions. MH500 [sample from the t(17;19) subject] RNA was processed using Ultraspec RNA (Biotecx, Houston, TX, BL-10⁻¹⁰⁰). Protein for reverse phase protein array was prepared as previously described (Kornblau et al., 2009).

Cell pellets from subject MH500 were prepared and karyotype and fluorescence in situ hybridization (FISH) analyses were performed as previously published (Poland et al., 2007).

KG-1 cells were cultured in Iscove's modified Dulbecco's medium (Gibco Life Technologies, Inc., Carlsbad, CA, 12200036) with 20% bovine growth serum (BGS; Hyclone, Logan, UT, SH30541.03) and U937 cells were cultured in RPMI 1640 (Gibco Life Technologies, Inc., 31800-022) with 10% BGS.

FISH

The t(17;19) translocation breakpoint regions were initially narrowed with directly labeled FISH probes as in Poland et al., 2007: LSI dual-color PML/RARA probe (Vysis, Abbott Park, IL, 32-191009) for 17q and the LSI dual-color to 19q13/19p13 probe (Vysis, 32-231004) for 19q. Indirectly labeled BAC FISH was performed as in Poland et al., 2007 with the following modifications: BACs RP11-380H7 and CTD-3149D2 were labeled with

biotin and used to mark the p-arm of chromosomes 17 and 19, respectively. The following probes, listed in order from centromere to telomere, were labeled with digoxigenin and used to map the translocation breakpoints; chromosome 17: RP11-506H21, RP11-110F1, RP11-113K1, RP11-112H10, RP11-481M4, RP11-118K23, RP11-561K8, RP11-721P9, CTB-61P23, RP11-489G5, RP11-52B5, RP11-90L11 and chromosome 19: RP11-84C16, RP11-568L16, RP11-43N16.

Primers

The sequences of the primers used in the following experiments can be found in Table 1.

Vectorette PCR

One microgram of genomic DNA from MH500 or U937 was digested with 20 units of BclI for 2 hr at 50°C. The Universal Vectorette System (Sigma-Genosys, St. Louis, MO, UVS1) was used to perform vectorette PCR. The vectorette library was created per the manufacturer's recommendation and half was diluted with 100 µl water. PCR was then performed using 2 µl of diluted library, a primer specific for exon 2 of *MPO* (*MPO* ex2), and the vectorette primer. The PCR product was diluted 1:100 with sterile water and 1 µl was used as the template for nested PCR with the nested exon 2 *MPO* primer (*MPO* n-ex2) and the nested vectorette primer. Bands unique to MH500 were gel purified using the QIAquick gel extraction kit (Qiagen, 28706), TOPO cloned into pCR2.1-TOPO (Invitrogen, Carlsbad, CA, K4550-01SC) and transformed into TOP10F' competent cells as recommended by the manufacturers. DNA from positive clones was prepared using the QIAprep spin miniprep kit (Qiagen, 27106) and sequenced.

Directed PCR

PCR was performed using genomic DNA from MH500 or the wild-type lymphoblastoid cell line (LCL) 4G3 and the following primer pairs surrounding the translocation breakpoints: *MPO*F + *ZNF342*R and *ZNF342*F + *MPO*R. The reaction contained 1× AccuTaq buffer, 2 mM dNTP, 200 ng template DNA, 2.5 µM each primer, and 2.5 U/µl AccuTaq polymerase (Sigma, St. Louis, MO, D8045). The PCR program was as follows: one cycle of 96°C for 2 min; 30 cycles of 94°C for 10 sec, 68°C for 1.5 min; one cycle of 68°C for 2 min. The PCR products were gel purified using QIAquick PCR purification kit (Qiagen, 28106) as recommended by the manufacturer and sequenced.

ZNF342 RNA Expression Analysis

SYBR green quantitative reverse transcriptase PCR (qRT-PCR) was performed for the following genes: *GEMIN7*, *CLPTM1*, *LOC284352*, *SFRS16*, *ZNF342*, *RELB*, *MPO*, *TRAPPC6A*, and *NKPD1*. Levels of expression were compared between MH500, three additional AML samples, one normal bone marrow, and KG-1 and U937 cell lines. The QuantiTect SYBR Green RT-PCR kit (Qiagen, 204143) was used and the 25 µl reaction contained 1× QuantiTect SYBR Green RT-PCR master mix, 1.6 µM each primer, 0.25 µl QuantiTect RT Mix, and 100 ng template RNA. The PCR program was as follows: one cycle of 50°C for 30 min; one cycle of 95°C for 15 min; 45 cycles of 95°C for 15 sec, 55°C for 30 sec, 72°C 30 sec. Each reaction was performed in triplicate for the gene of interest and *ACTB* for each patient sample.

To perform TaqMan qRT-PCR, cDNA was generated from 1 µg patient RNA using the high-capacity cDNA reverse transcription kit (Applied Biosystems, Foster City, CA, 4374966) with RNase inhibitor according to the manufacturer's recommendation. PCR (Applied Biosystems, 4304437) was performed in duplicate with 1 µl of cDNA and either primers for *ACTB* or *ZNF342* in a 25 µl reaction containing 1× TaqMan Universal PCR

Master Mix, 500 nM F primer, 500 nM R primer, and 250 nM TaqMan probe. The PCR program was as follows: one cycle of 50°C for 2 min; one cycle of 95°C for 10 min; 45 cycles of 95°C for 15 sec, 50°C for 1 min. The primers used are as follows: ACTB F, ACTB R, ACTB TaqMan, ZNF342 F, ZNF342 R, and ZNF342 TaqMan.

Quantitation of Murine Gene Expression

Mpo and *Zfp296* levels were based on published data from Chambers et al. (2007) quantitated in murine hematopoietic populations by RNA hybridization to Affymetrix (Santa Clara, CA) MOE430 2.0 microarrays as previously published (Chambers et al., 2007).

ZNF342 Sequencing

To sequence the three exons of the *ZNF342* gene we used four sets of primers, each set included M13F and M13R sequence: ex1F + ex1R, ex2F + ex2R, ex3 – 1F + ex3 – 1R, ex3 – 2F + ex3 – 2R. The reaction contained 1× GoTaq Flexi buffer, 2.5 mM MgCl₂, 0.2 mM dNTP, 0.5 mM F + R primer mix, 1.25U GoTaq polymerase (Promega, Madison, WI, M8291), 100 ng genomic DNA template, and 1 M betaine (Sigma, B0300). The PCR program was as follows: one cycle of 96°C for 2 min; 5 cycles of 95°C for 30 sec, 60°C for 30 sec, 72°C for 45 sec; 35 cycles of 95°C for 30 sec, 55°C for 30 sec, 72°C for 45 sec; one cycle of 72°C for 5 min. Reactions were sequenced using M13F and M13R primers.

Reverse Phase Protein Array Assembly and Printing Method

For quantification purposes, five serial dilutions (1:2 dilution steps) of each protein lysate were arrayed in 384 well plates (Genetix, Boston, Massachusetts). Samples were printed onto nitrocellulose coated glass slides (FAST Slides, Schleicher & Schuell BioScience, Inc. USA, Keene, NH) using an Aushon Biosystems 2470 Arrayer (Aushon BioSystems Inc., Burlington, MA) with 175 micron pins and a single touch. The samples were printed in replicate, printed side by side. Based on the sample concentration of 1×10^4 cells per microliter and a printing volume of 2 nanoliter/touch, we estimate that the spots ranged from 85 cell equivalents of protein in undiluted, with ~5 cell protein equivalents in the most diluted (1:16) spot. To permit topographical normalization, a sample of protein prepared from 11 pooled cell lines, printed in five serial dilutions or a negative control sample, was printed at the end of each row of patient sample, creating a grid across the whole slide. Each slide contained 6,912 dots.

Antibody Detection and Array Staining

A detailed description of the array methodology including antibody staining and detection has been published (Tibes et al., 2006) and the experiment was performed as published. A rabbit polyclonal antibody (AB) against ZNF342 (Abcam, Cambridge, MA, ab51265) at a concentration of 1:1,000 was added for 1–2 hr with frequent rotation. A biotinylated secondary antibody (anti-rabbit), diluted 1:15,000 and used for signal amplification, was added for 1 hr. Subsequently, the array slides were incubated using the DAKO (Copenhagen, Denmark) signal amplification system using catalyzed reporter deposition of substrate to amplify the signal detected by the primary antibody (Hunyady et al., 1996). Slides were incubated in streptavidine-biotin-peroxidase and biotinyl-tyramide/hydrogen peroxide reagents. Finally, 3,3'-diaminobenzidine tetrachloride (DAB) was cleaved by tyramide-bound horseradish peroxidase, giving a stable brown precipitate with excellent signal-to-noise ratio. This technique is sensitive and reproducible to the femtomolar range as reported (Charboneau et al., 2002; Tibes et al., 2006).

Survival Analysis

Survival analysis for RPPA data were performed using Statistica, version 6 (Statsoft, Tulsa, OK).

RESULTS

Case Report and Cytogenetic Evaluation

A previously healthy 10-year-old boy presented to Texas Children's Hospital with low grade fever, pallor, and enlarged lymph nodes. Peripheral blood counts included white blood cells, 5,500 per microliter, with 65% blasts. Cytogenetic analysis of a bone marrow specimen revealed 20/20 cells with 46, XY, t(17;19)(q23;q13) (Fig. 1) and 2/20 cells contained a deletion of the long arm of chromosome 7 (7q-) at band 7q22. The patient was diagnosed with acute myeloid leukemia (AML) subtype M1 and the parents gave informed consent to participate in St. Jude AML 2002 treatment trial and molecular hematology studies (sample MH500). A cytogenetic analysis of PHA-stimulated T-lymphocytes revealed a normal 46,XY karyotype in all cells examined (data not shown), confirming that the t(17;19) in the bone marrow was an acquired leukemic clone. After treatment the patient was t(17;19) and minimal residual disease negative. A relapse bone marrow sample showed the presence of the t(17;19) in 2/30 cells with additional secondary changes, but lacking the deletion of 7q present in a subset of the original blast population, pointing to the t(17;19) as the causative factor and not the 7q deletion. The patient received high dose chemotherapy and total body irradiation followed by allogeneic bone marrow transplantation from an unrelated female donor. The patient engrafted at day +18 and has remained completely chimeric for 39 months. The posttransplant course was complicated including pancytopenia associated with infection that responded to infusion of CD34+ donor stem cells.

Identification of Breakpoint Region

Review of cytogenetics databases did not reveal any other report of this translocation. Therefore, we embarked on more precisely mapping the breakpoints using iterative rounds of FISH probes that map to 17q and 19q. We performed FISH analysis on metaphase spreads from patient MH500 bone marrow using indirectly labeled BAC probes. The BACs RP11-380H7 and CTD-3149D2 were labeled with biotin (green signal) and used as controls in all experiments to mark the p-arm of chromosomes 17 and 19, respectively. The BACs used to narrow the translocation breakpoint region on the chromosomes' q-arms were labeled with digoxigenin (red signal). Green and red signals seen on the same chromosome indicated the q-arm BAC was centromeric to the breakpoint. The translocation of the red signal to a different chromosome indicated the q-arm BAC was telomeric to the breakpoint. For chromosome 17, we found that the BACs RP11-506H21 and RP11-110F1 hybridized centromeric and telomeric of the breakpoint, respectively, placing the break in a 67 kilobase (kb) region containing a single gene, *MPO* (Fig. 2A). For chromosome 19, we found that the BACs RP11-84C16 and RP11-568L16 hybridized centromeric and telomeric of the translocation breakpoint, respectively, placing the break in a 264 kb region containing 11 genes (Fig. 2B).

Identification of the Precise Breakpoint

Attempts to identify a fusion RNA transcript using multiple rounds of RACE-PCR for all of the genes in the breakpoint region failed (data not shown). Therefore, to more precisely map the breakpoint in the t(17;19) translocation, we performed vectorette PCR on genomic DNA from the bone marrow sample. This method can be used to determine the sequence of an unknown region adjacent to a known region, in this case the gene *MPO*. BclI vectorette libraries from the MH500 leukemia sample and the U937 cell line as a control were used as

the template for nested PCR using primers to exon 2 of *MPO* and the vectorette unit. The resulting PCR products found in MH500 but not the U937 cell line were sequenced. One band was found to contain DNA sequence from both chromosomes 17 and 19, suggesting that it derived from the translocation breakpoint. This product placed the breakpoint 451 base pairs (bp) 5' of *MPO* and 1916 bp 5' of *ZNF342* on the derivative chromosome 19 (Fig. 3A).

To confirm the location of the translocation breakpoint and to determine if there were any small duplications or deletions at the breakpoints, we performed directed PCR on MH500 genomic DNA using primers surrounding the putative breakpoints on both translocated chromosomes. Fusion PCR products containing chromosome 17 and 19 sequences were found only in the MH500 sample (Fig. 3B). The breakpoint on the derivative chromosome 19 is 451 bp 5' of *MPO* and 1916 bp 5' of *ZNF342*, as found with the vectorette PCR, but on the derivative chromosome 17 the breakpoint is 352 bp 5' of *MPO* and 2,085 bp 5' of *ZNF342*, demonstrating areas of shared sequence on both translocated chromosomes, 99 bp of chromosome 17 and 169 bp of chromosome 19 (Fig. 3C). This fine mapping placed the translocation at t(17;19)(q22;q13.32), a slightly different location than the t(17;19)(q23;q13) found in the original cytogenetics report from a bone marrow sample. We focused our further studies primarily on the derivative chromosome 17 to determine if close proximity of the well-described *MPO* transcriptional enhancers (Orita et al., 1997; Austin et al., 1998; Yao et al., 2008) translocated 5' of *ZNF342* resulted in its overexpression.

Quantitative Gene Expression

We performed quantitative SYBR Green RT-PCR to determine if one or more genes in the interval on chromosome 19 were misexpressed in the bone marrow sample. The gene from the 17q breakpoint, *MPO*, was included in the analysis. RNA isolated from the t(17;19) sample MH500 was compared with three additional pediatric AML samples, one normal bone marrow sample, and two leukemia cell lines, KG1 and U937. Of the nine genes tested, only *ZNF342* was overexpressed specifically in the MH500 patient sample (Table 2). This 90-fold overexpression is consistent with the model that translocation of the *ZNF342* gene and promoter region juxtaposed to the *MPO* promoter/enhancer region results in increased expression of *ZNF342* in myeloid leukemia cells.

Expression of *ZNF342* has only been previously reported in human embryonic stem cell lines (Zeng et al., 2004) and not included in most human microarray experiments. We researched array data for levels of *Mpo* and the ortholog *Zfp296* in murine hematopoietic cells (Fig. 4; Chambers et al., 2007). As expected, *Mpo* levels are the highest in granulocytes and erythrocytes. However, *Zfp296* has lower expression in those cell types and highest expression in B and T-cells. Thus, the translocation appears to result in both overexpression and a shift of the normal expression pattern of this zinc finger gene.

Mutational Analysis of *ZNF342* in Leukemia Samples

For many genes found at translocation breakpoints there is evidence for point mutations in other leukemia samples that can activate the protein. For example, the Janus kinase 2 (*JAK2*) can be activated by translocation (Peeters et al., 1997) or by point mutation (Jones et al., 2005). Therefore, we performed sequencing of the coding region of the *ZNF342* gene in a variety of leukemia samples: 22 adult AML samples, 1 adult ALL sample, 12 pediatric AML samples, 18 pediatric ALL samples, and 6 wild-type samples. The only sequence change identified was a heterozygous c.117C>A resulting in a D39E amino acid change found in 1 ALL and 2 AML pediatric samples for which no matched normal DNA was available to determine if this was a somatic change. This variant is absent from the dbSNP database so we performed directed sequencing of 100 control peripheral blood DNA

samples to determine if c.117C>A represents a benign polymorphism. Eight-nine samples had interpretable sequence traces and 1/89 contained the c.117C>A variant, which is most likely a single nucleotide polymorphism as it is found in >1% of the normal population. Thus, in this limited leukemia dataset, we find no evidence for somatic mutations in *ZNF342*.

Analysis of *ZNF342* mRNA and Protein Expression in Leukemia Samples

Review of an extensive cytogenetics database of 1727 adult leukemia samples at University of Texas MD Anderson Cancer Center revealed that 25 samples demonstrated add(19)(q13), suggesting that *ZNF342* might be overexpressed due to increased gene copy number. We performed TaqMan quantitative RT-PCR for *ZNF342* comparing MH500, two normal bone marrow samples, three leukemia samples with an add(19)(q13) karyotype, and five diploid AML samples. Comparison of the leukemia samples with the normal bone marrow showed variable expression with no significant increase of *ZNF342* in add(19)(q13) samples compared with diploid AML samples (Fig. 5). As expected, MH500 showed a high level of *ZNF342* overexpression.

We then determined *ZNF342* protein expression levels in a large number of AML ($n = 511$) and ALL ($n = 129$) samples using a previously described reverse phase protein array with linked clinical data (Kornblau et al., 2009). Comparing *ZNF342* levels in the top 3 quartiles of Philadelphia chromosome negative (PH-neg) ALL patients to the lower quartile, we determined that higher expression of *ZNF342* is associated with poorer survival in PH-neg ALL (Fig. 6) ($P = 0.033$). Our analysis of *ZNF342* levels in AML did not reveal a significant association with survival. The distribution of *ZNF342* levels in AML can be seen in Figure 7. There were a number of interesting observations for the 12 AML patients having greater than 2log2 increase in *ZNF342* expression compared with the mean. As described in Table 3, these patients with high *ZNF342* expression had a disproportionate number of *FLT3* internal tandem duplications (ITD) and AML M7 phenotype. DNA samples were not available to determine the mechanism of *ZNF342* overexpression in these cases.

DISCUSSION

The fine mapping of translocation breakpoints in AML has led to the identification of many genes important to the formation of leukemias. We have reported here a novel translocation t(17;19)(q22;q13.32) in AML that maps to 352 bp 5' of *MPO* on 17q and 2,085 bp 5' of *ZNF342* on 19q on the derivative chromosome 17.

The peroxidase reaction, staining for MPO activity, has been used as a leukemic diagnostic tool since 1910 (Fischel, 1910) and MPO staining has long been used by the World Health Organization (Vardiman et al., 2002) and the French-American-British Cooperative Group (Bennett et al., 1976) to help distinguish between AML and ALL and to subtype AMLs. Despite this analysis, there has never been a report of the *MPO* gene itself being directly involved in the formation of AML. Given the finding of this translocation in 100% of the leukemia blasts at diagnosis and in relapsed blasts and the overexpression of *ZNF342* in the leukemic cells, we propose that this *MPO*;*ZNF342* translocation plays a significant role in leukemia development in this patient. However, the *MPO* and *ZNF342* coding regions are not disrupted by the translocation, instead the break occurs in the promoter/enhancer region of both genes.

The *MPO* promoter/enhancer region has been extensively studied and contains multiple enhancers over a 5 kb interval including a granulocyte colony stimulating factor response element (GRE; Orita et al., 1997), two binding sites for AML1 (Austin et al., 1998; Yao et

al., 2008) and sites for C/EBP and c-Myb (Yao et al., 2008). On the derivative chromosome 17 the upstream enhancers (but not the basal promoter) are translocated 2 kb 5' of the gene *ZNF342* with SYBR green and TaqMan quantitative RT-PCR both demonstrating that *ZNF342* is highly overexpressed in the t(17;19) sample. This is the first reported case of a translocation in AML located in the promoter regions of both of the affected genes which does not result in a fusion transcript. Over-expression of the *CDX2* transcription factor causes AML in a murine model (Rawat et al., 2004); however, the translocation t(12;13) (p13;q12) associated with *CDX2* in human cancer did result in a *ETV6-CDX2* fusion transcript (Chase et al., 1999). Overall, chromosomal translocations associated with hematopoietic malignancies can be classified as resulting in either gene fusions or promoter/enhancer juxtapositions. The gene fusions result in production of a fusion transcript and/or protein, e.g., BCR-Abl (Hagemeijer et al., 1985). In contrast, the promoter/enhancer juxtapositions typically result in upregulation of one gene near the breakpoint by being placed in proximity to an active transcriptional unit on the other chromosome, e.g., Ig-*MYCC* (Erikson et al., 1982; la-Favera et al., 1982; Taub et al., 1982). Promoter/enhancer juxtaposition translocations are common in lymphoid malignancies, but the case described here suggests that similar molecular mechanisms can occur in myeloid malignancies.

We then performed initial analysis of *ZNF342* RNA and protein levels in a larger leukemia data-set which revealed that the highest 3 quartiles of *ZNF342* expression were associated with poorer survival in PH-neg adult ALL samples, a result that should be replicated in an independent data-set. Based on the murine expression data, *ZNF342* is normally expressed in the lymphoid lineage and this increased expression in ALL may not be the result of translocation but other transcriptional or posttranscriptional mechanisms. Although there was no prognostic impact of *ZNF342* expression in the total adult AML data-set, there were specific features of the small number of AML cases that had highest level of *ZNF342* protein expression including a significantly higher number of patients with FLT3-ITD and AML subtype M7. Future analyses in adult and pediatric AML samples could identify whether translocation or some other mechanism is responsible for overexpression of *ZNF342* in AML samples.

ZNF342 is known to be expressed in human embryonic stem cells although its transcriptional targets are not known (Zeng et al., 2004). Overexpression of *ZNF342* associated with translocation of the strong myeloid enhancers of *MPO* is analogous to the insertion of the strong constitutive retroviral promoter/enhancer elements at Evi82 causing *Zfp296* overexpression in the leukemic mice. Both lymphoid and myeloid leukemias are derived from retroviral insertions at Evi82 (Suzuki et al., 2002). Thus, overexpression of *ZNF342* by translocation or other mechanisms can contribute to leukemia formation in multiple hematopoietic compartments.

Acknowledgments

We gratefully acknowledge the collaboration and input from Dr. Margaret Goodell, Meghan Tierney and Dr. Eastwood Leung. D.L.S. was supported by Hematology Training Grant (T32 DK60445) and Molecular Medicine Scholars Program (T32HL066991). S.M.K. was supported by The Therapy of AML Core A Sample Distribution, Processing and Culture (2P01 CA55164-05A1).

Supported by: Hematology Training Grant, Grant number: T32 DK60445; Molecular Medicine Scholars Program, Grant number: T32HL066991; The Therapy of AML Core A Sample Distribution, Processing and Culture, Grant number: 2P01 CA55164-05A1.

References

- Arthur DC, Berger R, Golomb HM, Swansbury GJ, Reeves BR, Alimena G, Van Den Berghe H, Bloomfield CD, de la Chapelle A, Dewald GW. The clinical significance of karyotype in acute myelogenous leukemia. *Cancer Genet Cytogenet.* 1989; 40:203–216. [PubMed: 2766244]
- Austin GE, Zhao WG, Regmi A, Lu JP, Braun J. Identification of an upstream enhancer containing an AML1 site in the human myeloperoxidase (MPO) gene. *Leuk Res.* 1998; 22:1037–1048. [PubMed: 9783807]
- Bennett JM, Catovsky D, Daniel MT, Flandrin G, Galton DA, Gralnick HR, Sultan C. Proposals for the classification of the acute leukaemias. French-American-British (FAB) co-operative group. *Br J Haematol.* 1976; 33:451–458. [PubMed: 188440]
- Chambers SM, Boles NC, Lin KY, Tierney MP, Bowman TV, Bradfute SB, Chen AJ, Merchant AA, Sirin O, Weksberg DC, Merchant MG, Fisk CJ, Shaw CA, Goodell MA. Hematopoietic fingerprints: An expression database of stem cells and their progeny. *Cell Stem Cell.* 2007; 1:578–591. [PubMed: 18371395]
- Charboneau L, Tory H, Chen T, Winters M, Petricoin EF III, Liotta LA, Paweletz CP. Utility of reverse phase protein arrays: Applications to signalling pathways and human body arrays. *Brief Funct Genomic Proteomic.* 2002; 1:305–315. [PubMed: 15239896]
- Chase A, Reiter A, Burci L, Cazzaniga G, Biondi A, Pickard J, Roberts IA, Goldman JM, Cross NC. Fusion of ETV6 to the caudal-related homeobox gene CDX2 in acute myeloid leukemia with the t(12;13)(p13;q12). *Blood.* 1999; 93:1025–1031. [PubMed: 9920852]
- Dear TN. Cloning, structure, expression analysis, and assignment to mouse chromosome 7 of the gene Zfp296 encoding a zinc finger protein. *Mamm Genome.* 2000; 11:1037–1039. [PubMed: 11063263]
- Erikson J, Finan J, Nowell PC, Croce CM. Translocation of immunoglobulin VH genes in Burkitt lymphoma. *Proc Natl Acad Sci USA.* 1982; 79:5611–5615. [PubMed: 6813863]
- Fischel R. Der histochemisch Nachweis der Peroxydase. *Wiener Klin Wschr.* 1910; 223:1557–1558.
- Hagemeyer A, de KA, Godde-Salz E, Turc-Carel C, Smit EM, van Agthoven AJ, Grosveld GC. Translocation of c-abl to “masked” Ph in chronic myeloid leukemia. *Cancer Genet Cytogenet.* 1985; 18:95–104. [PubMed: 3863697]
- Hunyady B, Krempels K, Harta G, Mezey E. Immunohistochemical signal amplification by catalyzed reporter deposition and its application in double immunostaining. *J Histochem Cytochem.* 1996; 44:1353–1362. [PubMed: 8985127]
- Jones AV, Kreil S, Zoi K, Waghorn K, Curtis C, Zhang L, Score J, Seear R, Chase AJ, Grand FH, White H, Zoi C, Loukopoulos D, Terpos E, Vervessou EC, Schultheis B, Emig M, Ernst T, Lengfelder E, Hehlmann R, Hochhaus A, Oscier D, Silver RT, Reiter A, Cross NC. Widespread occurrence of the JAK2 V617F mutation in chronic myeloproliferative disorders. *Blood.* 2005; 106:2162–2168. [PubMed: 15920007]
- Kornblau SM, Tibes R, Qiu Y, Chen W, Kantarjian HM, Andreeff M, Coombes KR, Mills GB. Functional proteomic profiling of AML predicts response and survival. *Blood.* 2009; 113:154–164. [PubMed: 18840713]
- la-Favera R, Bregni M, Erikson J, Patterson D, Gallo RC, Croce CM. Human c-myc onc gene is located on the region of chromosome 8 that is translocated in Burkitt lymphoma cells. *Proc Natl Acad Sci USA.* 1982; 79:7824–7827. [PubMed: 6961453]
- Li J, Shen H, Himmel KL, Dupuy AJ, Largaespada DA, Nakamura T, Shaughnessy JD Jr, Jenkins NA, Copeland NG. Leukaemia disease genes: Large-scale cloning and pathway predictions. *Nat Genet.* 1999; 23:348–353. [PubMed: 10610183]
- Orita T, Shimozaki K, Murakami H, Nagata S. Binding of NF-Y transcription factor to one of the cis-elements in the myeloperoxidase gene promoter that responds to granulocyte colony-stimulating factor. *J Biol Chem.* 1997; 272:23216–23223. [PubMed: 9287329]
- Peeters P, Raynaud SD, Cools J, Wlodarska I, Grosgeorge J, Philip P, Monpoux F, Van Rompaey L, Baens M, Van Den Berghe H, Marynen P. Fusion of TEL, the ETS-variant gene 6 (ETV6), to the receptor-associated kinase JAK2 as a result of t(9;12) in a lymphoid and t(9;15;12) in a myeloid leukemia. *Blood.* 1997; 90:2535–2540. [PubMed: 9326218]

- Poland KS, Azim M, Folsom M, Goldfarb R, Naeem R, Korch C, Drabkin HA, Gemmill RM, Plon SE. A constitutional balanced t(3;8)(p14;q24.1) translocation results in disruption of the TRC8 gene and predisposition to clear cell renal cell carcinoma. *Genes Chromosomes Cancer*. 2007; 46:805–812. [PubMed: 17539022]
- Rawat VPS, Cusan M, Deshpande A, Hiddemann W, Quintanilla-Martinez L, Humphries RK, Bohlander SK, Feuring-Buske M, Buske C. Ectopic expression of the homeobox gene *Cdx2* is the transforming event in a mouse model of t(12;13)(p13;q12) acute myeloid leukemia. *Proc Natl Acad Sci USA*. 2004; 101:817–822. [PubMed: 14718672]
- Suzuki T, Shen H, Akagi K, Morse HC, Malley JD, Naiman DQ, Jenkins NA, Copeland NG. New genes involved in cancer identified by retroviral tagging. *Nat Genet*. 2002; 32:166–174. [PubMed: 12185365]
- Taub R, Kirsch I, Morton C, Lenoir G, Swan D, Tronick S, Aaronson S, Leder P. Translocation of the c-myc gene into the immunoglobulin heavy chain locus in human Burkitt lymphoma and murine plasmacytoma cells. *Proc Natl Acad Sci USA*. 1982; 79:7837–7841. [PubMed: 6818551]
- Tibes R, Qiu Y, Lu Y, Hennessy B, Andreeff M, Mills GB, Kornblau SM. Reverse phase protein array: Validation of a novel proteomic technology and utility for analysis of primary leukemia specimens and hematopoietic stem cells. *Mol Cancer Ther*. 2006; 5:2512–2521. [PubMed: 17041095]
- Vardiman JW, Harris NL, Brunning RD. The World Health Organization (WHO) classification of the myeloid neoplasms. *Blood*. 2002; 100:2292–2302. [PubMed: 12239137]
- Yao C, Qin Z, Works KN, Austin GE, Young AN. C/EBP and C-Myb sites are important for the functional activity of the human myeloperoxidase upstream enhancer. *Biochem Biophys Res Commun*. 2008; 371:309–314. [PubMed: 18435917]
- Zeng X, Miura T, Luo Y, Bhattacharya B, Condie B, Chen J, Ginis I, Lyons I, Mejido J, Puri RK, Rao MS, Freed WJ. Properties of pluripotent human embryonic stem cells BG01 and BG02. *Stem Cells*. 2004; 22:292–312. [PubMed: 15153607]

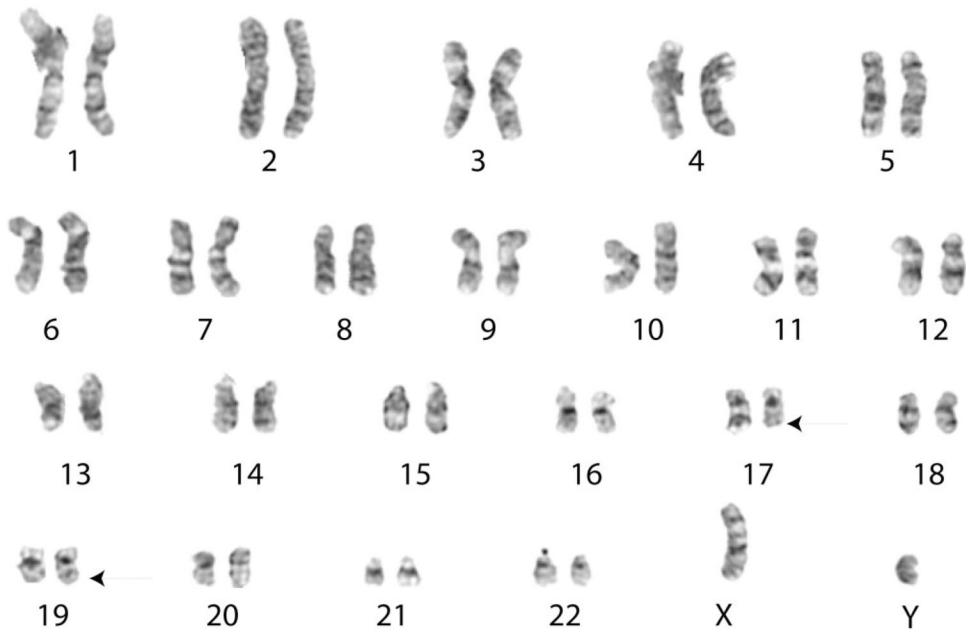


Figure 1. Karyotype analysis from MH500 at diagnosis showing the apparently balanced $t(17;19)(q23;q13)$ found in 20/20 bone marrow cells.

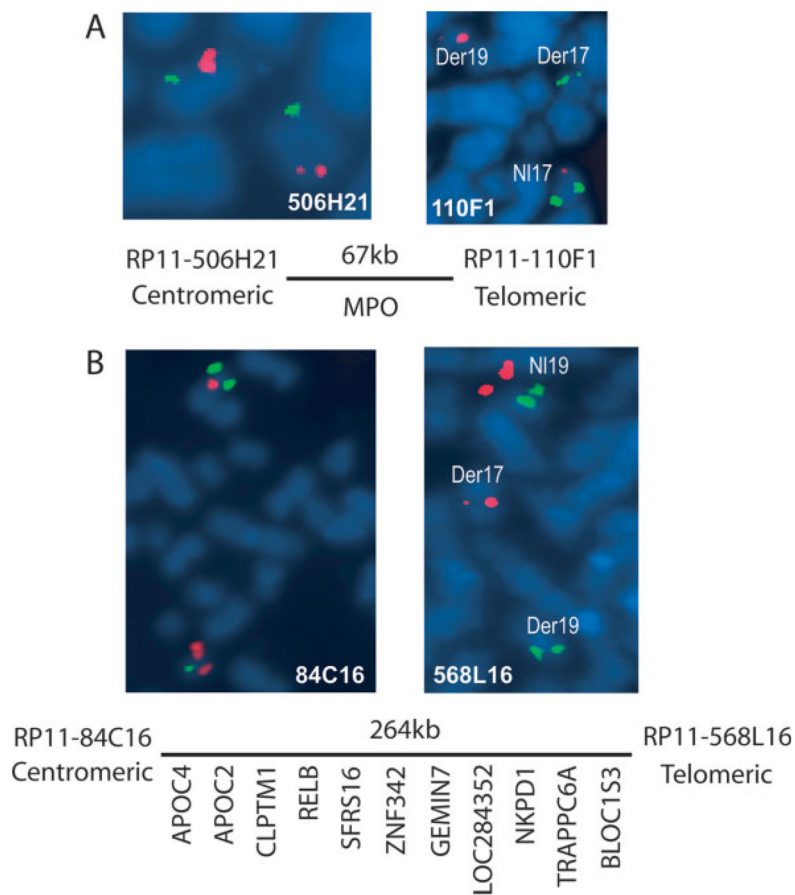


Figure 2. Mapping of the translocation breakpoint by FISH. Indirectly labeled BAC FISH probes were hybridized to metaphase spreads from MH500 blasts. The green signals represent BACs RP11-380H7 and CTD-3149D2, which were labeled with biotin and used to mark the p-arm of chromosomes 17 and 19, respectively. The red signals represent BACs labeled with digoxigenin and used to map the translocation breakpoints. The genes contained in the breakpoint interval are shown beneath the FISH data. A: The breakpoint region on 17q was narrowed to 67 kb (53,672,821–53,739,940) with the BAC RP11-506H21 centromeric to the breakpoint and the BAC RP11-110F1 telomeric to the breakpoint. B: The breakpoint region on 19q was narrowed to 264kb (50,122,986–50,386,821) with the BAC RP11-84C16 centromeric to the breakpoint and the BAC RP11-568L16 telomeric to the breakpoint.

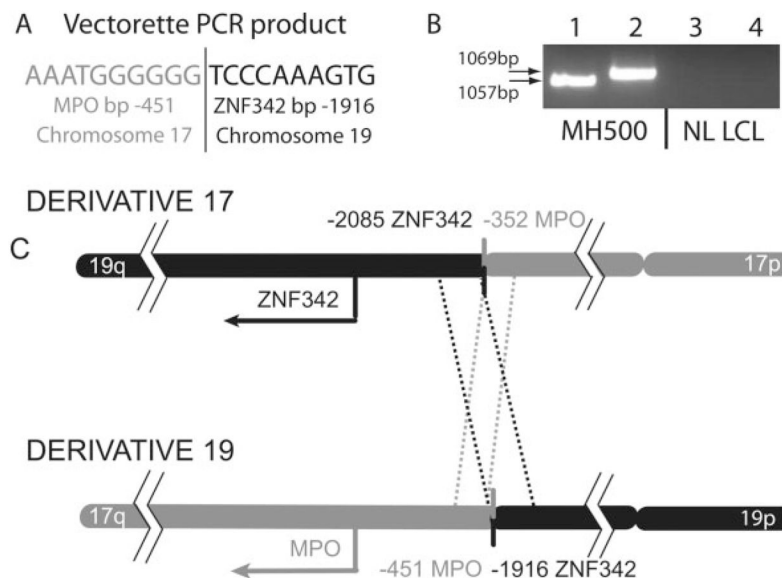


Figure 3. Precise breakpoint mapping with vectorette PCR and directed PCR. **A:** Partial sequence of the vectorette PCR product mapping the derivative 19 breakpoint to 451bp 5' of *MPO* on 17q and 1916bp 5' of *ZNF342* on 19q. **B:** Directed PCR confirming the presence of genomic fusion products and the breakpoint location in patient MH500 (lanes 1 and 2) compared with wild-type LCL 4G3 DNA (lanes 3 and 4). Lanes 1 and 3 using *MPO* F and *ZNF342* R primers, lanes 2 and 4 using *ZNF342* F and *MPO* R primers. **C:** Diagram of precise breakpoint mapping from sequencing of directed PCR. The derivative chromosome 17 breakpoint is located at 352bp 5' of *MPO* and 2085bp 5' of *ZNF342*. The derivative chromosome 19 breakpoint is located at 451bp 5' of *MPO* and 1916bp 5' of *ZNF342*. The dashed lines denote the DNA sequence found on both derivative chromosomes.

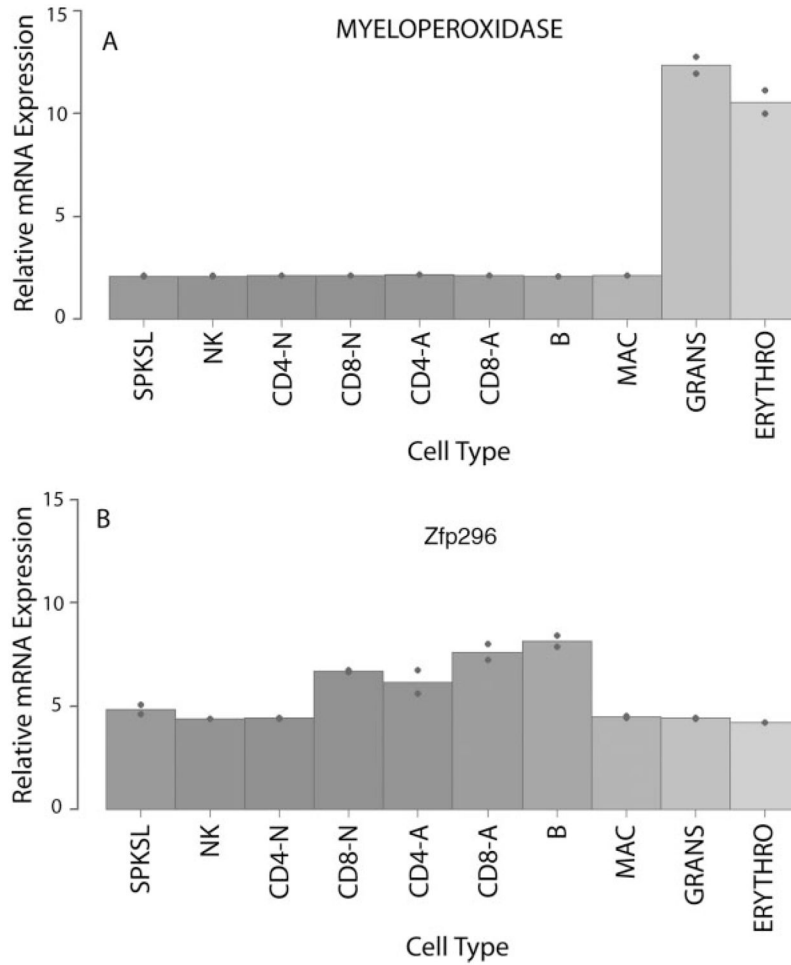


Figure 4. *Mpo* and *Zfp296* expression in normal murine hematopoietic cells. Normal murine hematopoietic stem cells (SPKSL), natural killer cells (NK), naïve CD4⁺ helper T-cells (CD4-N), naïve CD8⁺ cytotoxic T-cells (CD8-N), activated CD4⁺ helper T-cells (CD4-A), activated CD8⁺ cytotoxic T-cells (CD8-A), B-cells (B), macrophages (MAC), granulocytes (GRANS), and erythrocytes (erythro). A: *MPO* has the highest expression in granulocytes and erythrocytes. B: *Zfp296* has the highest expression in B and T-cells. Normalized (log₂) expression intensity obtained by querying dataset described in Chambers et al. (2007).

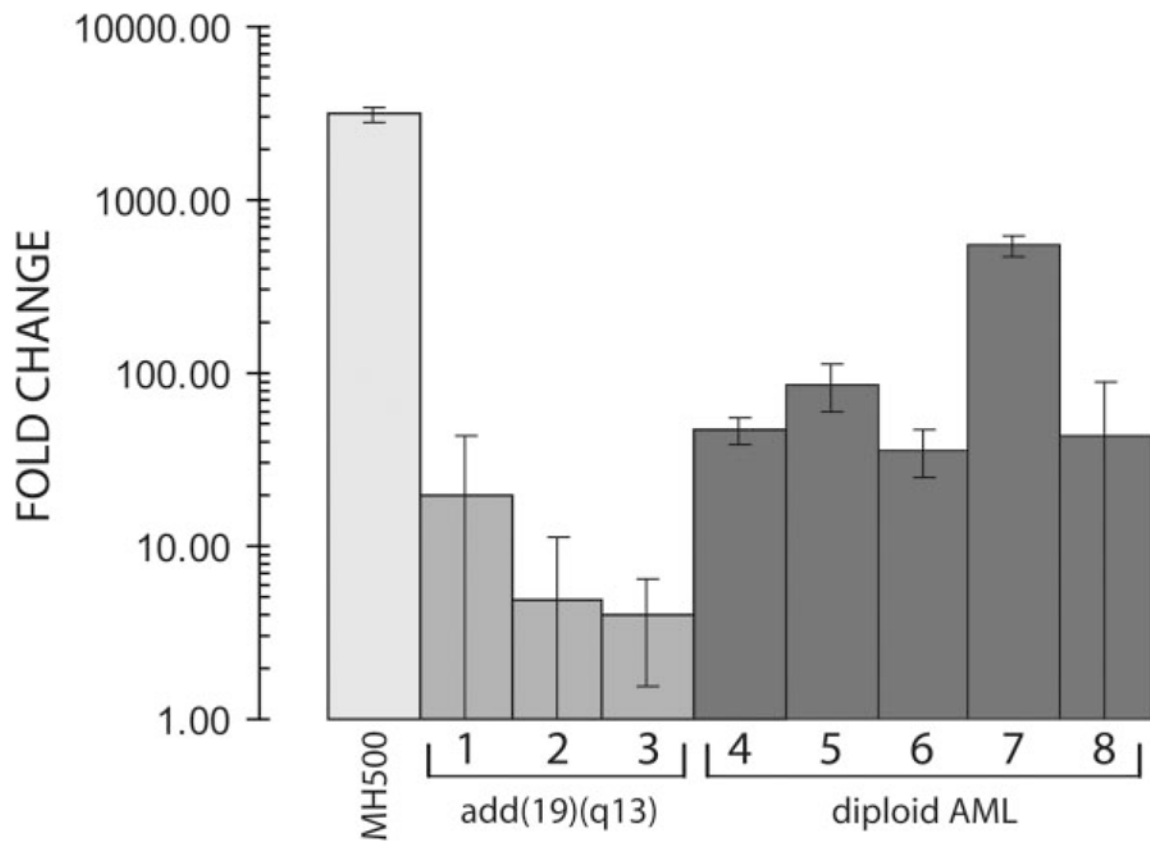


Figure 5. Expression of *ZNF342* in AML Samples. TaqMan qRT-PCR analysis of *ZNF342* confirming overexpression in MH500 and demonstrating a variable expression in additional leukemia samples, with no significant increase in *ZNF342* expression in samples containing an add(19)(q13) cytogenetic abnormality compared to diploid AMLs.

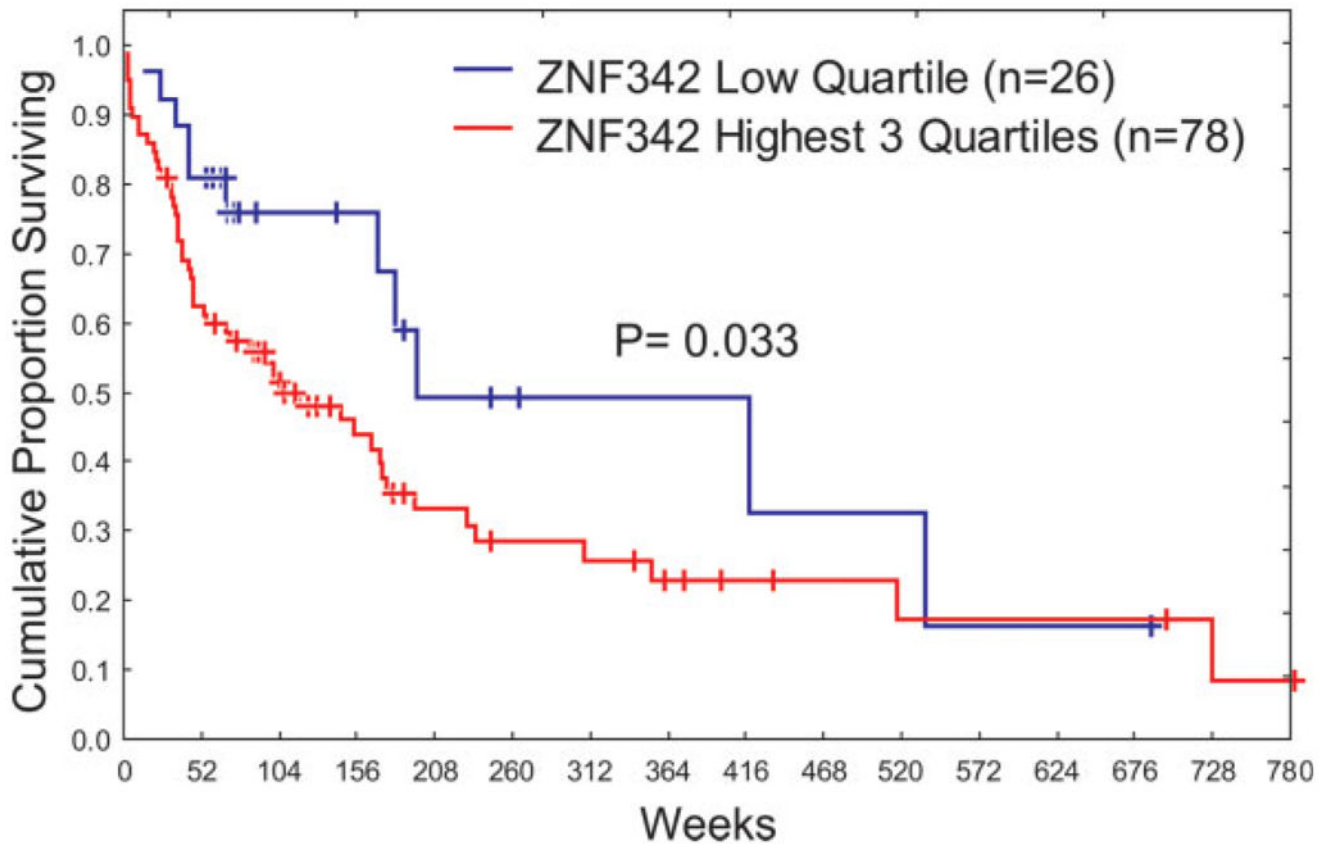


Figure 6.

The effect of ZNF342 level on overall survival in PH-neg ALL. Comparison of the protein levels of ZNF342 in the lowest quartile of Ph-negative ALL patients ($n = 26$) to the higher 3 quartiles ($n = 78$) reveals that higher ZNF342 levels significantly effect overall survival ($P = 0.033$). [Color figure can be viewed in the online issue, which is available at www.interscience.wiley.com.]

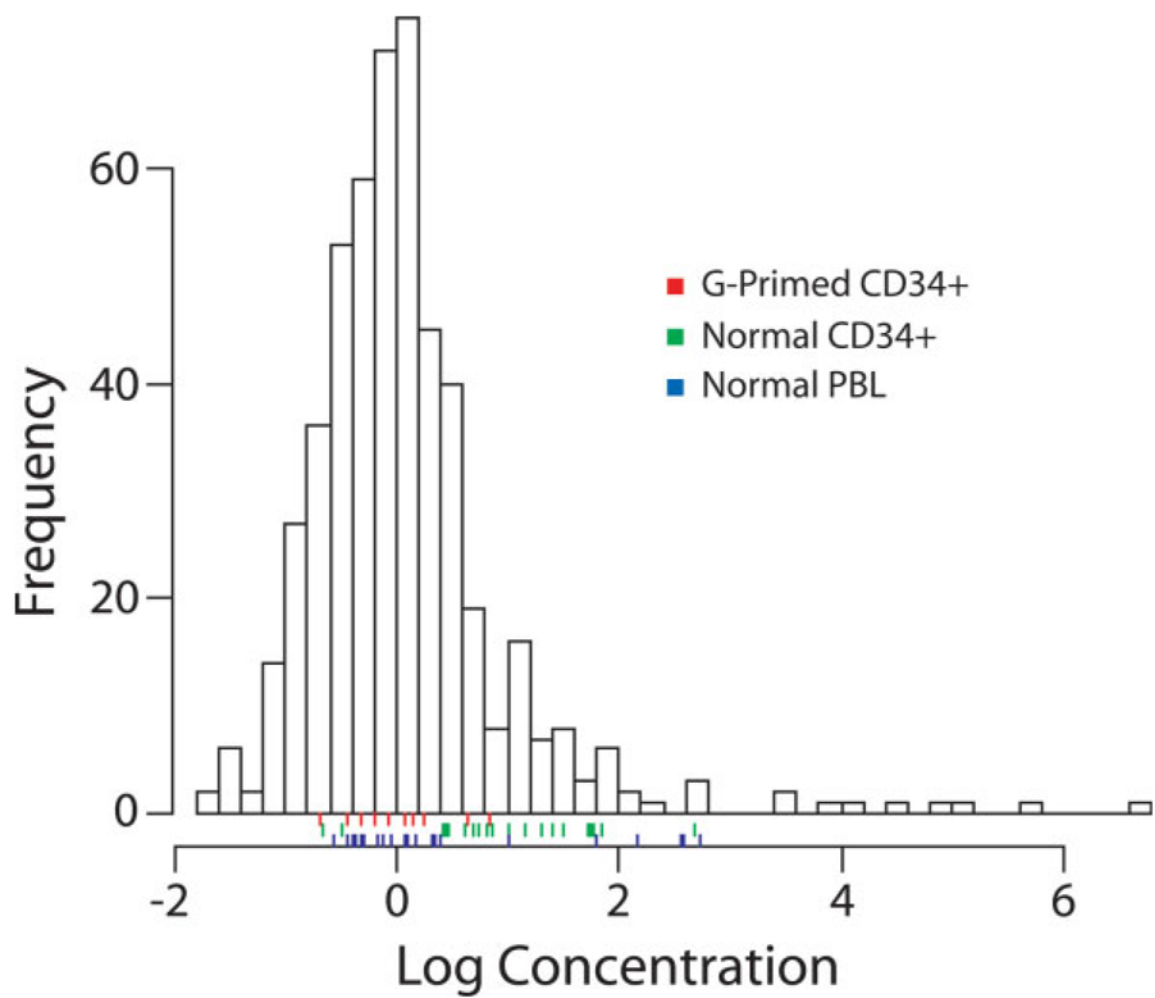


Figure 7. Distribution of ZNF342 protein expression in AML samples using RPPA. [G-Primed = CD34+ cells primed with granulocyte colony stimulating factor (G-CSF)]. [Color figure can be viewed in the online issue, which is available at www.interscience.wiley.com.]

TABLE 1

Experimental Primer Sequences

Primer	Experiment	Sequence
GEMIN7 F	SYBR Green qRT-PCR	CAGGAGGGAGCCAAGACAATG
GEMIN7 R	SYBR Green qRT-PCR	AAGCCACGGCTGAAGCCATCA
CLPTM1 F	SYBR Green qRT-PCR	GTTCTGGCCTTCAAGAATGA
CLPTM1 R	SYBR Green qRT-PCR	TCGTTGTCCAGGATGTAGAGG
LOC284352 F	SYBR Green qRT-PCR	CCACATGATGCGCAAGACGAG
LOC284352 R	SYBR Green qRT-PCR	CAGGCTGGCGTTCTCCAAGTG
SFRS16 F	SYBR Green qRT-PCR	GACGGTGACTTCGTCAGGATG
SFRS16 R	SYBR Green qRT-PCR	CATGGCCTTCTCCTCTCAAG
ZNF342 F	SYBR Green qRT-PCR	GAGGCCATCACTGCCTTCATG
ZNF342 R	SYBR Green qRT-PCR	CTCCAGGCCACTGTGAACTG
RELB F	SYBR Green qRT-PCR	GCCCGTCTATGACAAGAAATCCA
RELB R	SYBR Green qRT-PCR	CGGCGTCTTGAACACAATGGC
ACTB F	SYBR Green qRT-PCR	AGAGAGGCATCCTCACCCCTG
ACTB R	SYBR Green qRT-PCR	ATGAGGTAGTCAGTCAGGT
MPO F	SYBR Green qRT-PCR	TTGACAACCTGCACGATGAC
MPO R	SYBR Green qRT-PCR	TGTGCTCCCGAAGTAAGAG
TRAPPC6A F	SYBR Green qRT-PCR	GACCTACGTCCTGCAAGACAA
TRAPPC6A R	SYBR Green qRT-PCR	CGGAATCACCACTGGAACCTT
NKPD1 F	SYBR Green qRT-PCR	CGTGCTCAACGCCATCAACAC
NKPD1 R	SYBR Green qRT-PCR	AGTGCGGTTGAGGAAGAGGTA
MPO ex2	Vectorette PCR	CTTTCCCGCCGCTCCTTGTAGGC
MPO n-ex2	Vectorette PCR	GTCCACCAGCTGCTTGGCCTCCTC
MPO F	Directed PCR	CCCAGCCCAGCAAGGTCCTAAGTC
ZNF342 R	Directed PCR	CCTCCCTATTCCAGGCCAGTCAGAA
ZNF342 F	Directed PCR	GCCGCTCCTCTGATCACCTTTT
MPO R	Directed PCR	TCTTGGTCCTGCGCCACAGTC
ZNF342 ex1 M13F	ZNF342 sequencing	GTAAAACGACGGCCAGTGCCGCGAGTCACTCACCTG
ZNF342 ex1 M13R	ZNF342 sequencing	CAGGAAACAGCTATGACCGGCGAAGGAGATAAAGGCAG
ZNF342 ex2 M13F	ZNF342 sequencing	GTAAAACGACGGCCAGTTTCCCCTCTCCTTCAGCAC)
ZNF342 ex2 M13R	ZNF342 sequencing	CAGGAAACAGCTATGACCCTTTCCAGCAGGAAGCCC
ZNF342 ex3-1 M13F	ZNF342 sequencing	GTAAAACGACGGCCAGTCAGGAGTGCCTATCCCACAG
ZNF342 ex3-1 M13R	ZNF342 sequencing	CAGGAAACAGCTATGACCGGTTCTTGACACCTGCTG
ZNF342 ex3-2 M13F	ZNF342 sequencing	GTAAAACGACGGCCAGTGACACCAGCCAGGAGCAG
ZNF342 ex3-2 M13R	ZNF342 sequencing	CAGGAAACAGCTATGACCGAGGAGGTCATGGGTGTTG
ACTB F	Taqman qPCR	AGAGAGGCATCCTCACCCCTG
ACTB R	Taqman qPCR	ATCTTCATGAGGTAGTCAGTCAGGT
ACTB Taqman	Taqman qPCR	CCATCGAGCACGGCATCGTCA
ZNF342 F	Taqman qPCR	GAGGCCATCACTGCCTTCATG
ZNF342 R	Taqman qPCR	CTCCAGGCCACTGTGAACTG

Primer	Experiment	Sequence
ZNF342 Taqman	Taqman qPCR	AAGAAGCTGGGCTGTCAGCTCTTCAGA

TABLE 2

Relative mRNA Expression in MH500 AML Sample Compared with Normal Bone Marrow for Genes Near t(17;19) Breakpoint

	MH500
<i>MPO</i>	2.4
<i>CLPTM1</i>	3.7
<i>RELB</i>	0.3
<i>SFRS16</i>	7.4
<i>ZNF342</i>	91.8
<i>GEMIN7</i>	1.6
<i>LOC284352</i>	3.4
<i>NKPD1</i>	5.3
<i>TRAPPC6A</i>	2.8

TABLE 3Clinical Features of AML Patients with $>2\log_2$ ZNF342 Protein Expression Compared with the Entire Cohort

	ZNF342 <2	ZNF342 $2\log_2$	P-value	χ^2
N	499	12		
Subtype M7	8	2	0.0002	13.86
Male:Female	287:212	4:8	0.0950	2.79
Age (median)	65.75	64.79	0.8800	NA
Diploid Yes:No	206:293	7:5	0.2360	1.40
FLT3-ITD Yes:No	71:379	5:4	0.0016	9.23